

Supplementary Materials for

The evolution of anti-bat sensory illusions in moths

Juliette J. Rubin*, Chris A. Hamilton*, Chris J. W. McClure, Brad A. Chadwell, Akito Y. Kawahara*, Jesse R. Barber*

*Corresponding author. Email: julietterubin@boisestate.edu (J.J.R.); chamilton@flmnh.ufl.edu (C.A.H.); kawahara@flmnh.ufl.edu (A.Y.K.); jessebarber@boisestate.edu (J.R.B.)

Published 6 July 2018, *Sci. Adv.* **4**, eaar7428 (2018)
DOI: 10.1126/sciadv.aar7428

The PDF file includes:

Fig. S1. Twisted and cupped hindwing tail ends in Saturniidae.

Fig. S2. Hindwing morphology of the three silk moth species was altered by cutting and gluing hindwing material.

Fig. S3. IPI does not change on the basis of moth treatment.

Fig. S4. IPI does not change on the basis of moth genus or hindwing length.

Fig. S5. ASR demonstrates multiple origins of the hindwing tail trait within the Saturniinae subfamily.

Fig. S6. ASR demonstrates multiple origins of adaptive peaks within the Saturniinae subfamily.

Table S1. Kinematic output results from 100 ms of tethered moth flight leading up to bat-moth interaction.

Table S2. Bat identity and experience (that is, learning) do not affect the outcome of the trial.

Table S3. Bats do not change call parameters during attack on silk moths of differing morphologies.

Legends for movies S1 to S7

Other Supplementary Material for this manuscript includes the following:

(available at advances.sciencemag.org/cgi/content/full/4/7/eaar7428/DC1)

Movie S1 (.mov format). Phylomorphospace by tail regime.

Movie S2 (.mov format). Phylomorphospace by tail regime (no labels).

Movie S3 (.mov format). Phylomorphospace by adaptive peak.

Movie S4 (.mov format). Phylomorphospace by adaptive peak (no labels).

Movie S5 (.mov format). Bat attack on elongated hindwing lobes.

Movie S6 (.mp4 format). Bat attack on intact hindwing tails.

Movie S7 (.mp4 format). Bat attack on intact tail ends.

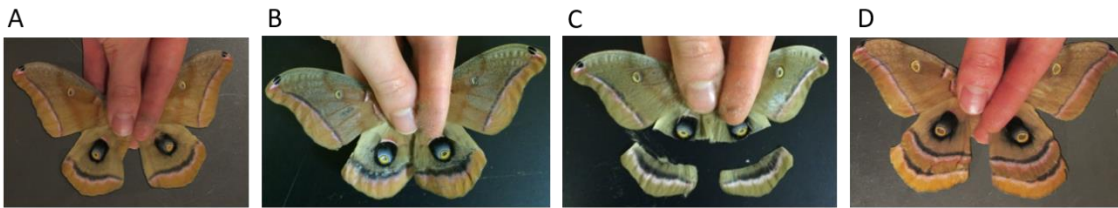
SUPPLEMENTARY MATERIALS

FIGURES:

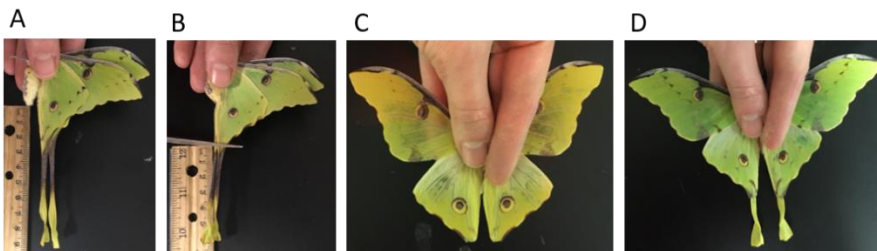


Fig. S1. Twisted and cupped hindwing tail ends in Saturniidae. (A) *Copiopteryx semiramis* (Arsenurinae, Arsenurini), (B) *Eudaemonia argiphontes* (Saturniinae, Urotini), (C) *Titaea tamerlan* (Arsenurinae, Arsenurini), (D) *Coscinocera hercules* (Saturniinae, Saturniini), (E) *Graellsia isabellae* (Saturniinae, Saturniini), (F) *Actias luna* (Saturniinae, Saturniini), (G) *Actias maenas* (Saturniinae, Saturniini), (H) *Actias isis* (Saturniinae, Saturniini).

Antheraea polyphemus



Argema mimosae



Actias luna



Fig. S2. Hindwing morphology of the three silk moth species was altered by cutting and gluing hindwing material. All *A* photos are intact representatives, *B* photos are the control “sham” treatment, where hindwing material was cut as if to ablate and then re-glued to the same animal. Photo *C* is shortened in *Antheraea polyphemus*, and ablated in *Argema mimosae* and *Actias luna*, to remove hindwing tails. Photo *D* of *A. polyphemus* is elongated, where hindwing lobes from another polyphemus are glued to the ends of an intact moth’s hindwings. Photo *D* of *A. mimosae* is shortened, where hindwing tails are shortened by removing the tail shafts and regluing the twisted and cupped ends to the base of the hindwings. Photos *D* and *E* of *A. luna* are shortened and blunt, respectively. These variants have the same hindwing length, although the length is made up of twisted and cupped tail ends in shortened luna and simple shafts in blunt luna. Photo *F* of *A. luna* photo is elongated, where whole tails from one luna moth were attached to the shafts of another. Background color was photoshopped in intact polyphemus, elongated polyphemus, and blunt luna pictures.

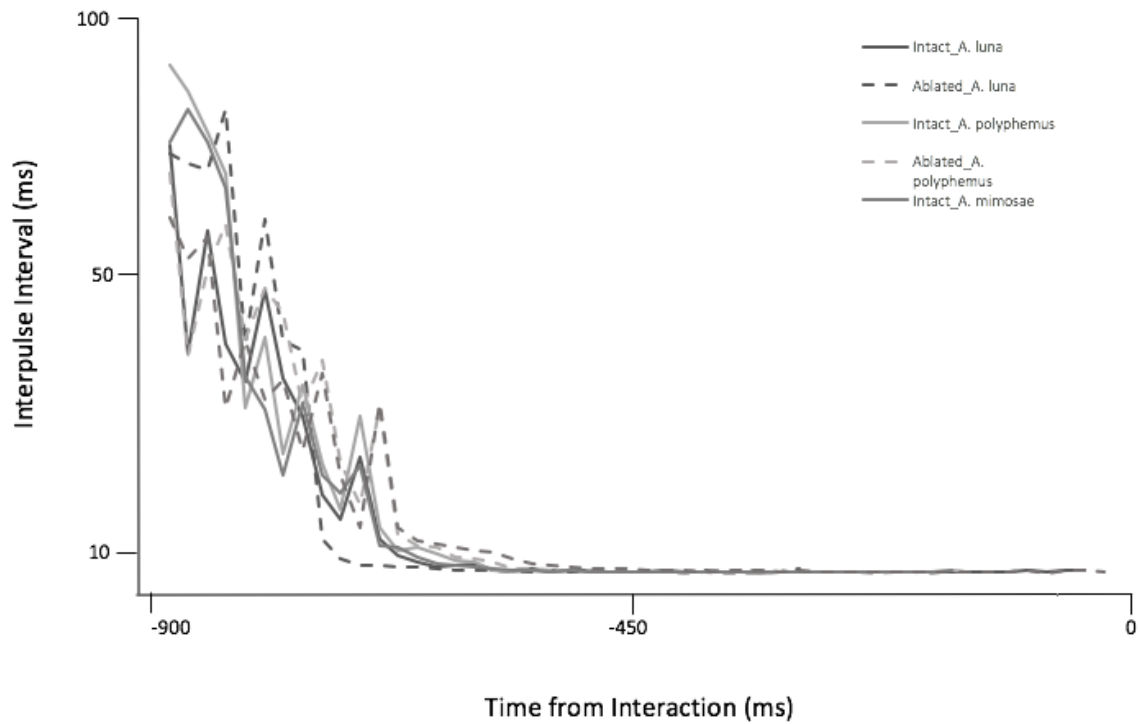


Fig. S3. IPI does not change on the basis of moth treatment. One representative echolocation call sequence against an individual moth from intact and ablated treatments of *Actias luna*, and intact and shortened treatments of *Antheraea polyphemus*, highlighting that interpulse interval (time between the bat's emitted sonar pulses) does not change between tailed and non-tailed moths. Only one complete call sequence for these select treatments is depicted for viewing clarity. See fig. S4 for call sequences against all moth treatment types. Sonar analysis commences 900ms before interaction.

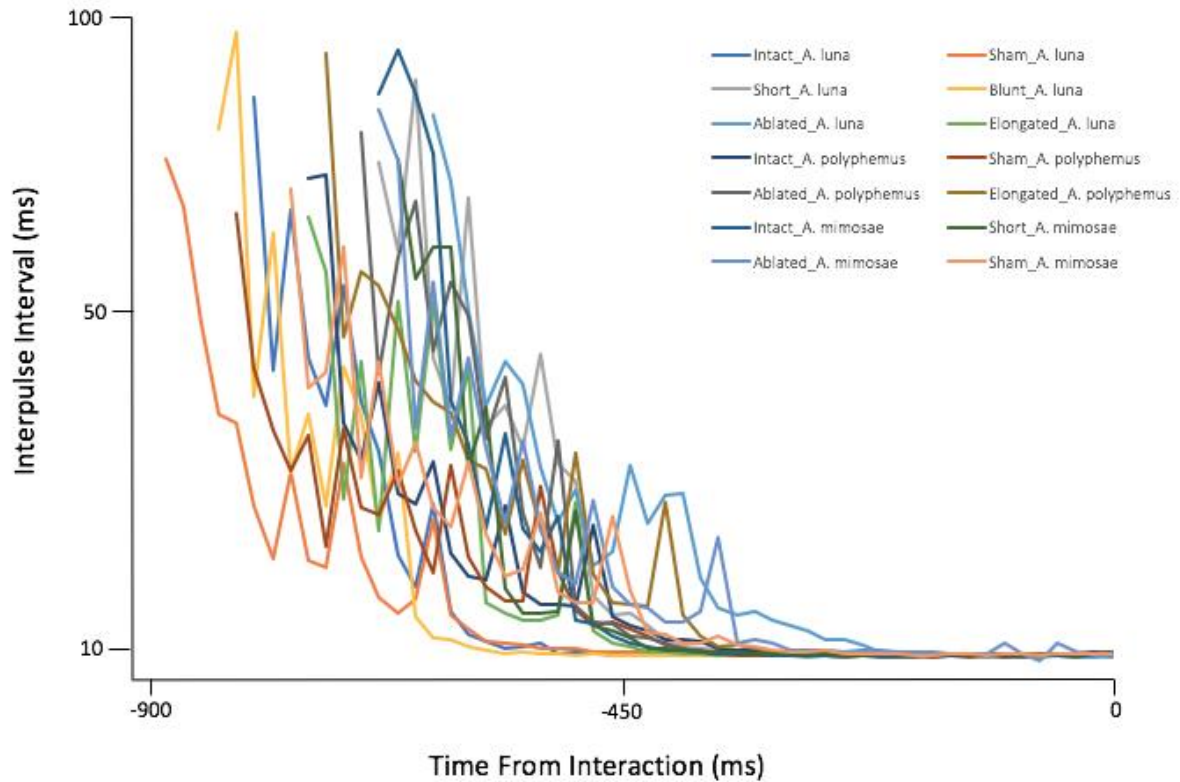


Fig. S4. IPI does not change on the basis of moth genus or hindwing length. One representative echolocation call sequence against an individual moth from each treatment, highlighting that there is no difference in interpulse interval (IPI) of bat attack based on moth genus or tail length. Sonar analysis commences 900ms before interaction.

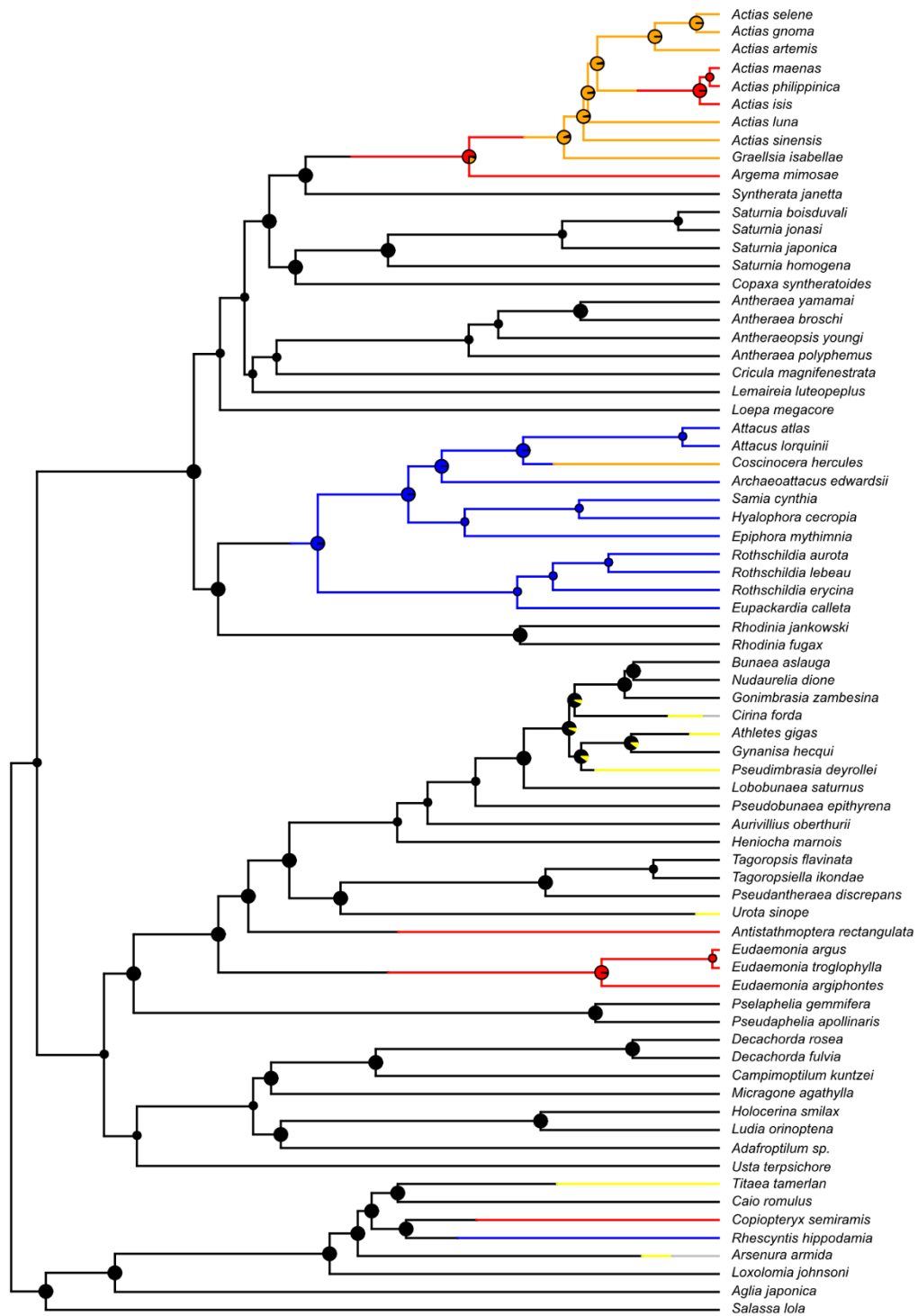


Fig. S5. ASR demonstrates multiple origins of the hindwing tail trait within the Saturniinae subfamily. Ancestral character state reconstruction (ASR) of hindwing shape categories demonstrates strong support that hindwing tails evolved at least 8 times within, and multiple times outside of, the Saturniinae. Elongated hindwing lobes also evolved twice in the Saturniidae, among the Attacini (Saturniinae) and in *Rhescyntis* (Arsenurinae). Terminal states are colored at the tips of their branch. Hindwing shape character states: extra-long tail (red); long tail (orange); short tail (yellow); elongated HW lobes (blue); graded HW extension (grey). Pie charts at internal nodes represent character state likelihoods, with black indicating a non-tailed ancestral state.

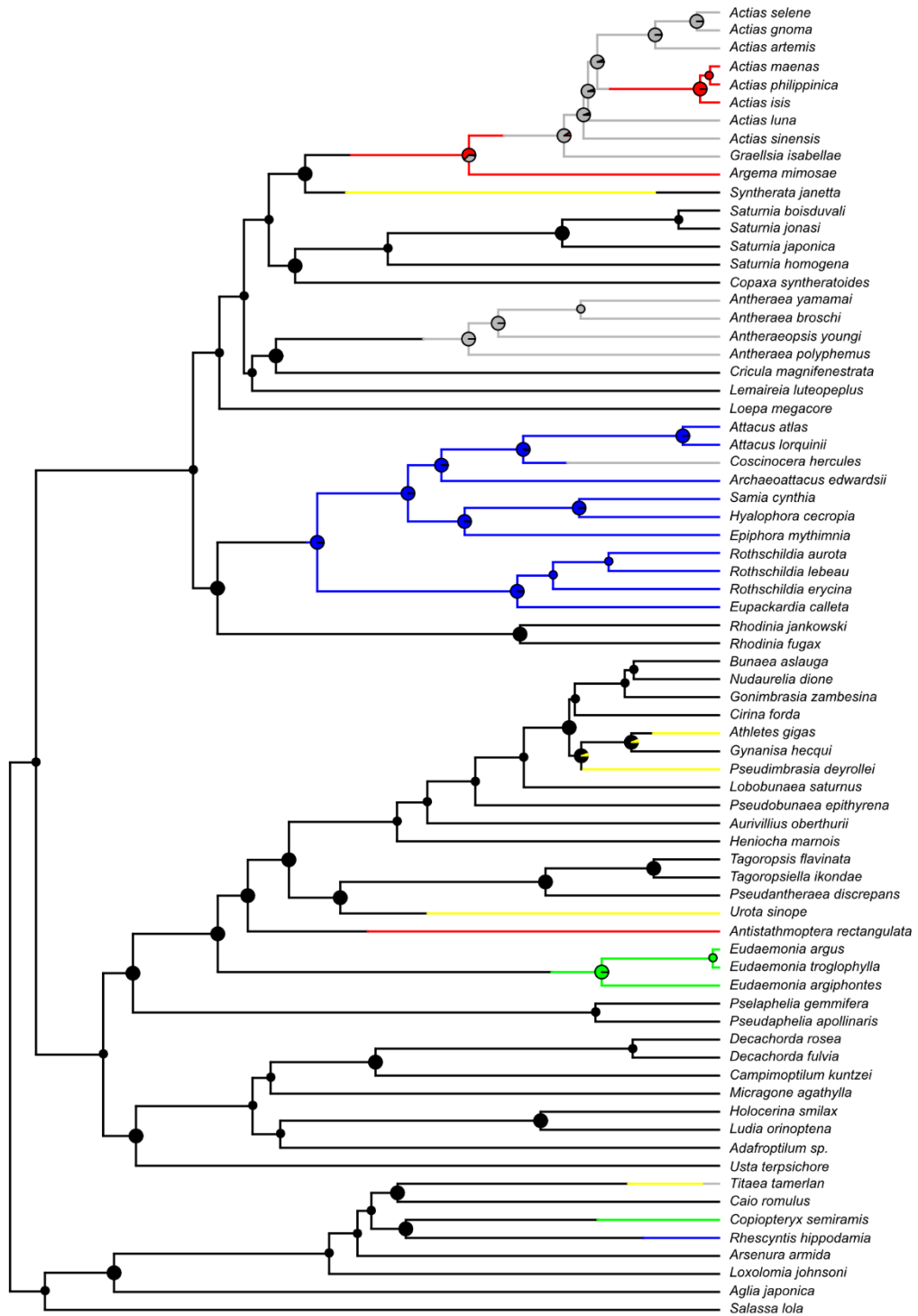


Fig. S6. ASR demonstrates multiple origins of adaptive peaks within the Saturniinae subfamily. Ancestral character state reconstruction (ASR) of *SURFACE* shape space regimes provide strong support that adaptive peaks have evolved at least 10 times within the Saturniinae, several via convergent evolution. Terminal states are colored at the tips of their branch. Character states: adaptive peak 1 (red) = extra-long tail; adaptive peak 2 (green) = extra-long tail; adaptive peak 3 (yellow) = short tail; adaptive peak 4 (blue) = elongated HW lobes; non-convergent adaptive peaks (grey). Including the outgroups, two additional convergence events can be identified – adaptive peak 2: extra-long tails in the Saturniinae and the Arsenurinae, and adaptive peak 4: extended HW lobes in the Attacini tribe (Saturniinae) and the genus *Rhescyntis* (Arsenurinae). Pie charts at internal nodes represent character state likelihoods, with black indicating a non-tailed ancestral state.

TABLES:

Table S1. Kinematic output results from 100 ms of tethered moth flight leading up to bat-moth interaction. Parameters in the table were highly correlated ($r_{ho}>0.7$) with mean curvature, radial acceleration, and tortuosity. Flight variables from each treatment compared with intact standards of the same species, outlined in black. Mean angular velocity of shortened *Argema mimosae* is the only parameter different from its intact counterpart (highlighted in red), although our Bayesian models revealed that this did not affect escape success or model slope.

	Mean Speed	Mean Tangential Acceleration	Mean Angular Velocity
Intact <i>A. mimosae</i>	mean=0.721 SD=(±0.096)	mean=0.029 SD=(±0.199)	mean=2.948 SD=(±0.61)
Sham <i>A. mimosae</i>	mean=0.845 SD=(±0.113)	mean=-0.141 SD=(±0.234)	mean=2.77 SD=(±0.713)
Shortened <i>A. mimosae</i>	mean=0.639 SD=(±0.097)	mean=-0.327 SD=(±0.198)	mean=4.72 SD=(±0.607)
Ablated <i>A. mimosae</i>	mean=0.475 SD=0.101	mean=-0.221 SD=(±0.208)	mean=3.119 SD=(±0.638)
Intact <i>A. luna</i>	mean=0.732 SD=(±0.101)	mean=-0.281 SD=(±0.209)	mean=4.066 SD=(±0.639)
Sham <i>A. luna</i>	mean=0.876 SD=(±0.093)	mean=-0.202 SD=(±0.191)	mean=3.631 SD=(±0.582)
Shortened <i>A. luna</i>	mean=0.902 SD=(±0.089)	mean=-0.165 SD=(±0.184)	mean=5.026 SD=(±0.56)
Blunt <i>A. luna</i>	mean=0.829 SD=0.101	mean=-0.721 SD=(±0.209)	mean=3.926 SD=(±0.637)
Ablated <i>A. luna</i>	mean=0.76 SD=0.101	mean=-0.121 SD=(±0.208)	mean=4.993 SD=(±0.637)
Elongated <i>A. luna</i>	mean=0.939 SD=0.101	mean=0.042 SD=(±0.208)	mean=4.608 SD=(±0.636)
Intact <i>A. polyphemus</i>	mean=0.671 SD=(±0.101)	mean=-0.122 SD=(±0.209)	mean=3.765 SD=(±0.638)
Sham <i>A. polyphemus</i>	mean=0.575 SD=(±0.101)	mean=-0.175 SD=0.208	mean=3.04 SD=(±0.637)
Ablated <i>A. polyphemus</i>	mean=0.661 SD=(±0.089)	mean=-0.024 SD=(±0.183)	mean=4.901 SD=(±0.558)
Elongated <i>A. polyphemus</i>	mean=0.686 SD=0.097	mean=0.089 SD=(±0.199)	mean=3.286 SD=(±0.607)

Table S2. Bat identity and experience (that is, learning) do not affect the outcome of the trial. Bat identities included as random intercepts, and the number of nights bats spent hunting silkmoths (bat experience) included as random slopes in a Bayesian model both overlap 0, indicating that they do not have an effect on moth escape success from bats.

Bat Experience		Bat Identity	
Bat	Overlap 0	Bat	Overlap 0
2C	TRUE	2C	TRUE
2M	TRUE	2M	TRUE
Artemis	TRUE	Artemis	TRUE
Bolt	TRUE	Bolt	TRUE
Bullfrog	TRUE	Bullfrog	TRUE
Chomper	TRUE	Chomper	TRUE
Devil	TRUE	Devil	TRUE
Dodge	TRUE	Dodge	TRUE
Jackie	TRUE	Jackie	TRUE
Jackie 2	TRUE	Jackie 2	TRUE
Lotus	TRUE	Lotus	TRUE
Marbles	TRUE	Marbles	TRUE
Nelly	TRUE	Nelly	TRUE
Snickers	TRUE	Snickers	TRUE
Squirt	TRUE	Squirt	TRUE
Stitch	TRUE	Stitch	TRUE

Table S3. Bats do not change call parameters during attack on silk moths of differing morphologies. Across moth treatments, there was no difference in average interpulse interval (IPI) during the buzz phase, “Buzz IPI” (slope of the line IPI versus tail length (cm) = -0.05 ± 0.04 , Overlap 0=TRUE); overall duration of buzz phase of the attack sequence, “Buzz Duration” (slope of buzz duration versus tail length (cm) = -0.04 ± 0.04 , Overlap 0=TRUE); or the lower frequency limit of the call, “15dB Below” (slope frequency 15dB below versus tail length (cm) = 0.00 ± 0.03 , Overlap 0=TRUE), measured as the frequency at 15 dB below the frequency at peak amplitude during the buzz.

	Buzz IPI (ms)	Buzz Duration (ms)	15dB below (kHz)
Intact <i>A. mimosae</i>	7.5 ± 0.5	120 ± 30	18.0 ± 1.1
Sham <i>A. mimosae</i>	7.6 ± 0.4	160 ± 40	18.5 ± 0.8
Shortened <i>A. mimosae</i>	7.7 ± 0.2	140 ± 20	17.6 ± 1.5
Ablated <i>A. mimosae</i>	8.0 ± 0.3	150 ± 40	18.1 ± 0.91
Intact <i>A. luna</i>	7.8 ± 0.4	170 ± 30	18.8 ± 1.4
Sham <i>A. luna</i>	8.0 ± 0.7	130 ± 50	19.1 ± 1.7
Shortened <i>A. luna</i>	7.8 ± 0.4	160 ± 70	17.3 ± 1.9
Blunt <i>A. luna</i>	7.8 ± 0.8	140 ± 50	18.4 ± 1.0
Ablated <i>A. luna</i>	8.0 ± 1.0	140 ± 40	18.6 ± 1.7
Elongated <i>A. luna</i>	8.0 ± 0.5	160 ± 60	18.4 ± 1.5
Intact <i>A. polyphemus</i>	8.0 ± 0.4	180 ± 80	19.0 ± 1.3
Sham <i>A. polyphemus</i>	7.8 ± 0.7	160 ± 70	18.9 ± 1.2
Ablated <i>A. polyphemus</i>	7.6 ± 0.5	130 ± 30	17.6 ± 1.1
Elongated <i>A. polyphemus</i>	7.8 ± 0.5	150 ± 30	17.7 ± 1.5

VIDEOS:

Movie S1. Phylomorphospace by tail regime. Three-dimensional, phylogenetically-corrected PCA (pPCA) phylomorphospace where the tangled web of branches highlights the convergent evolutionary path of these lineages into similar morphospace, with terminal states colored by their defined hindwing tail categories. Tip labels identify individual lineages, as in Fig. 1 and fig. S5. The first three PCs explain 94.7% of the shape variance analyzed. Character states: extra-long tail (red), long tail (orange); short tail (yellow); elongated HW lobes (blue); graded HW extension (grey).

Movie S2. Phylomorphospace by tail regime (no labels). Three-dimensional, phylogenetically-corrected PCA (pPCA) phylomorphospace; same as movie S1, with the removal of tip labels for ease of viewing.

Movie S3. Phylomorphospace by adaptive peak. Three-dimensional phylogenetically-corrected PCA (pPCA) phylomorphospace where the tangled web of branches highlights the convergent evolutionary path of these lineages into similar morphospace, with terminal states colored to represent the four convergent adaptive peaks identified by *SURFACE*. Tip labels provide identification, as in Fig. 1 and fig. S6. The first three PCs explain 94.7% of the shape variance analyzed. Character states: adaptive peak 1 (red) = extra-long tail; adaptive peak 2 (green) = extra-long tail; adaptive peak 3 (yellow) = short tail; adaptive peak 4 (blue) = elongated HW lobes; NC adaptive peaks (grey).

Movie S4. Phylomorphospace by adaptive peak (no labels). Three-dimensional phylogenetically-corrected PCA (pPCA) phylomorphospace; same as movie S3 without tip labels for ease of viewing.

Movie S5. Bat attack on elongated hindwing lobes. Bat aiming (contact, no capture) at the hindwing of a polyphemus moth with elongated HW treatment.

Movie S6. Bat attack on intact hindwing tails. Bat aiming at the hindwing/tail (second section, highlighted in green in Fig. 4B) of an intact moon moth, then an intact luna moth. Both videos depict a tail rip, which rarely occurred (intact moon moth tail rip = 7% of interactions, intact luna moth tail rip = 9% of interactions).

Movie S7. Bat attack on intact tail ends. Bat aiming at the twisted and cupped tail end (third section, highlighted in purple in Fig. 4B) of an intact moon moth, then an intact luna moth. Interaction with the moon moth depicts aim behavior with bat employing a wing flick strategy, while interaction with luna moth depicts aim and miss behavior with bat employing a summersault strategy.